Real-time holography in ruthenium-doped bismuth sillenite crystals at 1064 nm

Vera Marinova,[1,2] **Ren Chung Liu,**[1] **Shiuan Huei Lin,**[3] **and Ken Yuh Hsu**[1]

[1]*Photonics Department, National Chiao Tung University, Hsinchu 30050, Taiwan*
[2]*Institute of Optical Materials and Technologies, Bulgarian Academy of Science, Sofia 1113, Bulgaria*
[3]*Department of Electrophysics, National Chiao Tung University, Hsinchu 30050, Taiwan*
**Corresponding author: vmarinova@optics.bas.bg*

Received February 11, 2011; revised April 1, 2011; accepted April 16, 2011;
posted April 18, 2011 (Doc. ID 142337); published May 23, 2011

Real-time holographic recording and an improvement of the response time in ruthenium (Ru)-doped $Bi_{12}SiO_{20}$ (BSO) crystal at 1064 nm is obtained. Using green light pre-exposure, a significant operation speed of 60 ms is achieved. In addition, the ability for image reconstruction is demonstrated in Ru-doped BSO, supporting further applications as reversible media for real-time image processing at the near-IR spectral range. © 2011 Optical Society of America

OCIS codes: 090.5694, 160.5320, 210.4770.

In recent years, special attention in photorefractive crystals research has been focused on the materials' near-IR (NIR) sensitivity improvement and holographic recording speed optimization. The possibility to utilize cheap diode lasers in photorefractive devices development as well as noninvasive and *in situ* biomedical objects testing has become of essential technological interest [1,2]. Together with $BaTiO_3$ [3] and recently reported Te-doped $Sn_2P_2S_6$ crystals [4], sillenites are one of the best inorganic materials for real-time image processing and related dynamic applications [5]. They are already implemented in many devices, especially for nondestructive interferometric testing and acousto-optical imaging of biological tissues [6,7]. In 2001 [8], a compact and portable holographic interferometer using a $Bi_{12}SiO_{20}$ (BSO) crystal as a recording medium was assembled in various metrological systems. Furthermore, a multiwavelength holographic recording with multimode diode lasers was demonstrated using $Bi_{12}TiO_{20}$ (BTO) for applications in profilometry and surface analysis [9,10].

So far, a direct holographic recording at 1064 nm was possible only on undoped sillenites under an external electric field. Odulov *et al.* [11] reported an enhancement of the beam-coupling coefficient in undoped BTO after pre-exposure with visible (VIS) light. Later on, the pre-exposure process was used to control electron–hole competition at 780 nm, allowing a long lifetime of the recorded hole-based grating [12]. A possibility to achieve a subsecond response time at 810 and 980 nm was successfully demonstrated in BSO by increasing the oxygen defects concentration (oxygen deficiency) during the crystal growth process, e.g., by controlling the intrinsic defects in a crystal lattice [13]. Another way to improve the photorefractive performance and photosensitivity is to introduce suitable doping elements into the sillenite structure. We found that ruthenium (Ru) is an appropriate dopant that significantly improves the photosensitivity of BTO crystals [14,15]. Moreover, Ru addition shows prospective features for energy transfer and two-beam coupling efficiency enhancement in BSO as demonstrated by Ramaz *et al.* [16]. The authors reported very high photorefractive gain measured at 647 nm at the diffusion regime.

In this Letter, we present the response time and sensitivity enhancement of Ru-doped BSO at the NIR spectral range (1064 nm). We show that pre-excitation with an optical energy close to the energy level of the main photorefractive defect center typical for sillenites can improve the response time by a factor of 50. To the best of our knowledge, Ru is the first dopant in a sillenite-type crystal structure that shows significant recording speed and sensitivity at 1064 nm. The ability for image reconstruction is demonstrated, supporting prospect for further applications in real-time image processing analysis.

Ru-doped BSO crystal studied in this work was grown from stoichiometric solutions by the Czochralski method [17], and fully facetted crystals with excellent optical homogeneity were obtained. The Ru concentration of $6.1 \times 10^{18}\ \mathrm{cm}^{-3}$ in the grown crystal was determined by atomic absorption spectrometry. For holographic tests, a cube with rectangular dimensions 10.3 mm × 11.4 mm × 6.4 mm along (110), (1-10), and (001) crystallographic directions was prepared.

In the holographic experiments, a diode-pumped laser operating at 1064 nm was used to write gratings in a two-wave beam interference setup in transmission geometry, and the setup is shown in Fig. 1. The intensity of each recording beam was about $150\ \mathrm{mW/cm^2}$ and 30° of the writing angle outside the crystal. The development of the recorded grating was probed in real time with a low-power third beam from the same laser source. The diffracted light was measured with an Si detector located behind the crystal. For pre-exposure, 532 nm cw light from a Verdi laser source (adjustable intensity) was used for 5 min irradiation, and IR recording started immediately after it. The sample was thermally annealed before the experiments.

For the image reconstruction experiment, the described setup was slightly modified. The signal beam carries the magnified image of the mask, which is detected by the CCD camera (640 × 480 pixels), and the image is reconstructed by the reference beam.

Figure 2 shows the absorption spectrum of Ru-doped BSO. Comparison with nondoped BSO is also presented for reference. Obviously, with the addition of Ru, the main absorption edge is shifted to the red spectral range,

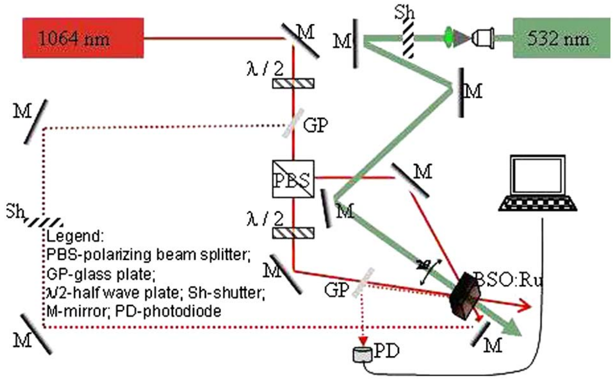

Fig. 1. (Color online) Experimental setup at 1064 nm: holographic recording and probing at real time. Green light is used only for pre-excitation.

which, along with the long wavelength tail, may be ascribed to absorption by Ru-related defects.

Moreover, a broad NIR absorption peak (with rather low intensity) is detected with a maximum around 1320 nm, suggesting further image processing possibilities at telecommunication wavelengths. As proposed by Oberschmid [18], the absorption shoulder of nondoped BSO, reaching out to ~480 nm, can be attributed to an intrinsic antisite defect formed by the occupation of a tetrahedrally coordinated Si^{4+} site by a Bi ion (known as a $\mathrm{Bi}_{\mathrm{Si}}$ center). Upon illumination, an electron (assumed n-type photoconductivity) can be excited to the conduction band (CB), leaving behind a hole-trapped defect forming a so-called $(\mathrm{Bi}^{3+}{}_{\mathrm{Si}} + h)$ center, confirmed by magnetic resonance spectroscopy [19]. This antisite Bi defect, located 2.2 eV below the CB at room temperature [19] (2.4 eV below the CB at liquid helium temperature [16]), is connected to the $\mathrm{Bi}^{3+}/\mathrm{Bi}^{4+}$ donor level as a main photorefractive defect and could be used as a primary source of photoelectrons in related light-induced effects, which requires further study. Direct detection by electron paramagnetic resonance demonstrated [20] that Ru doping results in $(\mathrm{Bi}^{3+}{}_{\mathrm{Si}} + h)$ centers already in the as-grown crystal, and this dopant introduces electron accepting levels close to the valence band (VB).

Because the optical excitation energy for the deep centers of the BSO:Ru crystal is roughly located close to 2 eV, we used it for pumping the main photorefractive level in the BSO structure. Figure 3 shows the recording and erasure processes at 1064 nm after green light exposure and comparison with the nonexposure sample at the first few seconds of the recording. Once the crystal is irradiated, significant improvement of the recording speed is detected and the writing kinetics shows very fast growth with a response time of 60 ms in a diffusion regime. The inset displays the recording and erasure dynamics without pre-exposure for a time scale necessary for the sample to reach the saturation state.

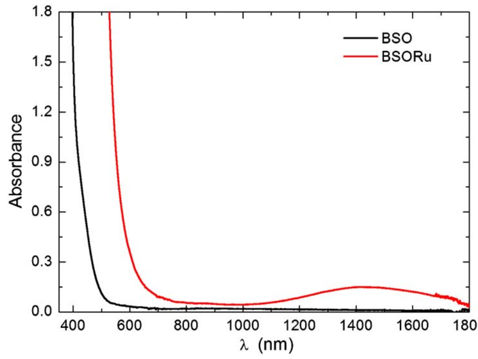

Fig. 2. (Color online) Optical absorption spectra of BSO:Ru compared to nondoped BSO at the VIS and NIR spectral range.

The detected diffracted signal is rather weak, however, it is in good agreement with the previously reported values for sillenites [3,4] when no external electric field is applied. Optically pumping the electrons using gating light is a recognized method to enhance the beam coupling gain [21] and improve the sensitivity [11]. Similar response time data of 130 ms in a BSO crystal using 810 nm has been reported by Raita *et al.* [13]. The measured subsecond operation speed is explained by high concentration of stoihiomertic defects, in particular by a significant amount of Si deficiency, which generates oxygen vacancies.

Figure 4 shows the response time dependence on the pump green light intensity for 5 min of illumination per measurement. The higher the average intensity used, the faster the measured response time. The response time behavior shows a tendency to saturate, although we could not use the highest available laser intensity in order to protect the sample.

It is well known that sillenites have a complex crystal structure that allows the existence of a number of charge-trapping sites. Usually, transition metal ions, due to the availability of d-electrons and/or an empty d-orbital, can take several valence states and might introduce both deep and shallow levels in a bandgap. Evidence of Ru-related high-density trap levels (positioned shallower than the deep levels typical for sillenites), acting as acceptor centers for photoexcited electrons, was demonstrated by a photo-induced absorption study [22]. By using magnetic circular dichroism (MCD), [16] demonstrated that Ru^{n+} substitute Bi sites in the pseudo-octahedron position (formed by Bi and oxygen atoms) under three valence states. Usually, Ru^{4+} possesses an amphotetic behavior; therefore, it can accept holes or electrons to produce Ru^{5+} or Ru^{3+}, respectively.

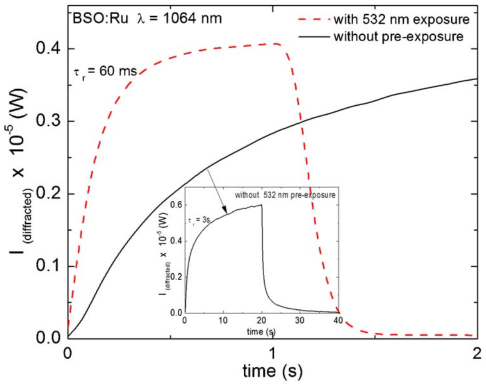

Fig. 3. (Color online) Dynamics of the recording and erasure processes of BSO:Ru at 1064 nm after 250 mW/cm^2 green light pre-exposure (dashed curve) and comparison with the nonexposure sample (solid curve) at the beginning of the recording. Inset: recording–erasure cycle without pre-exposure treatment.

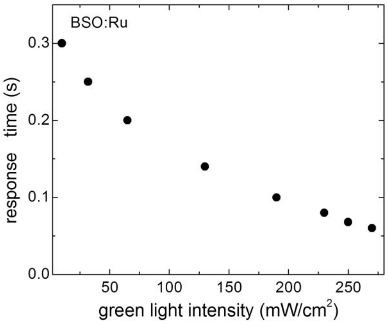

Fig. 4. Ru-doped BSO: response time (at 1064 nm) dependence on the pre-exposure light intensity of 532 nm.

In general, Ru can occur simultaneously in two or more valence states among which some may appear only after appropriate illumination. Therefore, the above presented holographic results correlate quite well with the MCD spectra at the NIR range measured in [16]. The thermally bleached Ru-doped BSO sample shows a sharp peak at 1.16 eV (1064 nm), which increased rapidly after red light illumination (the authors supposed the formation of Ru^{3+} and Ru^{5+} rising the concentration), supporting further feasibility for NIR sensitivity. Subsequent illumination with 2.75 eV (blue light) form paramagnetic $\mathrm{Bi_{Si}}^{4+}$ via the ionization of $\mathrm{Bi_{Si}}^{3+}$, which could be associated with the gating light pre-excitation of the main defect level during holographic recording and related response time enhancement. A schematic diagram of possible Ru levels, shallow traps, and the main PR center (deep defects) are presented in [5,16].

We suppose that the addition of Ru introduces trap levels, located between the Fermi level and CB (or VB), which improves the NIR sensitivity and opens further enhancement opportunities by controlling the valence state of Ru. Using green light pre-excitation, the charge carriers are excited and fill out those levels. Subsequent 1064 nm recording is carried out by electron excitation between previously filled levels (during the pre-excitation) and CB (assuming *n*-type conductivity), which improves the response time. Furthermore, an oxidation or reduction treatment process may change the type and number of the relevant defect levels and could give additional improvement in the reported values.

In addition, to reveal the NIR sensitivity of Ru-doped BSO, a reconstruction image test is demonstrated. The quality of image evolution is detected for different time scales, depending on the reconstructed beam and pre-exposure intensities. Figure 5 shows the time evolution of the reconstructed images taken by CCD camera.

In summary, we have demonstrated that Ru addition in a sillenite structure acts as a very effective trap center, which improves the sensitivity and response speed in the NIR. Furthermore, Ru-doped BSO shows prospective features for real-time analysis applications and image processing for nondestructive imaging of biocells and two-wavelength recording. The response time values could be improved further by oxidation/reduction treatments.

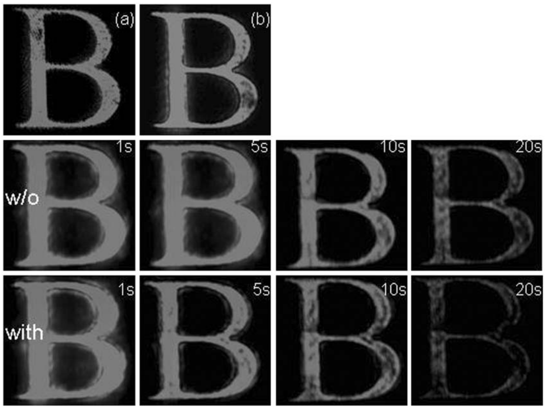

Fig. 5. Image reconstruction evolution in the Ru-doped BSO crystal at 1064 nm: (a) original image, (b) pass through the crystal. The next two rows show image development without (w/o) and with 532 nm pre-exposure, recorded at the same conditions (time of recording and reconstructed beam intensity).

Financial support from the National Science Council of Taiwan (NSCT) under contracts NSC 99-2911-1-009-008 and NSC 97-2628-E-009-034-MY3 is gratefully acknowledged. The sample was grown by the Crystal Growth Laboratory of the Institute of Solid State Physics, Sofia, supported by the Bulgarian National Fund project TK-X-1715/07.

References

1. P. Gunter and J.-P. Huignard, eds., in *Photorefractive Materials and Their Applications 3* (Springer, 2007).
2. S. Kober, J. Prauzner, M. Salvador, F. B. Kooistra, J. C. Hummelen, and K. Meerholz, Adv. Mater. **22**, 1383 (2010).
3. C. H. Lin, C. Y. Huang, and J. Y. Chang, Appl. Surf. Sci. **208–209**, 340 (2003).
4. R. Mosimann, P. Marty, T. Bach, F. Juvalta, M. Jazbinsek, P. Gunter, and A. Grabar, Opt. Lett. **32**, 3230 (2007).
5. J. Frejlich, *Photorefractive Materials* (Wiley, 2007).
6. E. A. Barbosa, A. O. Preto, D. M. Silva, J. F. Carvalho, and N. I. Morimoto, Opt. Commun. **281**, 408 (2008).
7. G. Caroena, M. Mori, M. R. R. Gusualdi, E. A. Liberti, E. Ferrara, and M. Muramatsu, J. Biomech. **43**, 680 (2010).
8. M. P. Georges, V. S. Scauflaire, and P. C. Lemare, Appl. Phys. B **72**, 761 (2001).
9. E. A. Barbosa, Appl. Phys. B. **80**, 345 (2005).
10. E. A. Barbosa, R. Verzini, and J. F. Carvalho, Opt. Commun. **263**, 189 (2006).
11. S. G. Odoulov, K. V. Shcherbin, and A. N. Shumeljuk, J. Opt. Soc. Am. B **11**, 1780 (1994).
12. P. V. dos Santos, J. Frejlich, and J. F. Carvalho, Appl. Phys. B **81**, 651 (2005).
13. E. Raita, O. Kobozev, A. A. Kamshilin, and V. V. Prokofiev, Opt. Lett. **25**, 1261 (2000).
14. V. Marinova, M. L. Hsieh, S. H. Lin, and K. Y. Hsu, Opt. Commun. **203**, 377 (2002).
15. V. Marinova, S. H. Lin, V. Sainov, M. Gospodinov, and K. Y. Hsu, J. Opt. A: Pure Appl. Opt. **5**, S500 (2003).
16. F. Ramaz, L. Rakitina, M. Gospodinov, and B. Briat, Opt. Mater. **27**, 1547 (2005).
17. P. Sveshtarov and M. Gospodinov, J. Cryst. Growth **113**, 186 (1991).
18. R. Oberschmid, Phys. Status Solidi A **89**, 263 (1985).
19. H. J. Reyher, U. Hellwig, and O. Thiemann, Phys. Rev. B **47**, 5638 (1993).
20. I. Ahmad, V. Marinova, and E. Goovaerts, Phys. Rev. B **79**, 033107 (2009).
21. A. Delboulbe, C. Fromont, J. P. Herriau, S. Mallick, and J.-P. Huignard, Appl. Phys. Lett. **55**, 713 (1989).
22. V. Marinova, I. Ahmad, and E. Goovaerts, J. Appl. Phys. **107**, 113106 (2010).